Journal of Environmental Chemical Engineering 5 (2017) 5588–5598

Contents lists available at ScienceDirect

Journal of Environmental Chemical Engineering

journal homepage: www.elsevier.com/locate/jece

Research paper

Process simulation, parametric sensitivity analysis and ANFIS modeling of CO_2 capture from natural gas using aqueous MDEA–PZ blend solution

Chikezie Nwaoha[a,*], Kenneth Odoh[b,*], Emmanuel Ikpatt[c], Rita Orji[d], Raphael Idem[a]

[a] Clean Energy Technologies Research Institute (CETRI), Faculty of Engineering and Applied Science, University of Regina, SK S4S 0A2, Canada
[b] University of Regina, SK S4S 0A2, Canada
[c] Process Systems Engineering Department, Cranfield University, United Kingdom
[d] Dalhousie University, Halifax, Nova Scotia, Canada

ARTICLE INFO

Keywords:
CO_2 capture
Natural gas
ProMax® 4.0 simulation
Methyldiethanolamine (MDEA)
Piperazine (PZ)
Adaptive neuro–fuzzy inference system (ANFIS)

ABSTRACT

Carbon dioxide (CO_2) capture from natural gas is integral towards meeting pipeline sales gas specifications and avoiding operational problems during natural gas liquefaction. Therefore, it is important to understand how different process parameters would affect the performance of the CO_2 capture process plant. In this research, CO_2 capture from a typical Nigerian natural gas composition was simulated using ProMax® 4.0. The validated simulation was used to generate 3125 datasets while varying a number of process parameters. A parametric sensitivity analysis was conducted by varying lean amine flow rate (LAF, 3500–4300 t/day), lean amine temperature (LAT, 40–60 °C), lean amine pressure (LAP, 60–75 bar), MDEA–PZ concentration difference ($C_{MDEA-PZ}$, 36–44 wt.%) and heat duty (HD, 50.4–56.52 GJ/h) to determine their effects on CO_2 capture efficiency alongside foaming and amine vaporization. The parametric analysis showed that the LAF and MDEA–PZ concentration have the highest effect on the CO_2 capture plant. In addition, 70% of the generated datasets was used to train the intelligent model named adaptive neuro–fuzzy inference system (ANFIS) while 30% was used for validation. Results revealed that the ANFIS model accurately predicted the simulation results with 2.4%AAD and RMSE of 4.0E-03, respectively.

1. Introduction

Utilization of low carbon fuels like natural gas will play a key role in reducing global carbon emissions. According to the British Petroleum (BP) Energy Outlook in 2016, the demand for natural gas grew by 1.8% per annum which made it the fastest growing fossil fuel [1]. In addition, it has been forecasted that the demand for natural gas will increase from 3160.2 million tonnes oil equivalent in 2015 to 4428.1 million tonnes oil equivalent in 2035 [1]. Therefore, natural gas transportation through pipeline and as liquefied natural gas (LNG) is expected to increase. The extraction of CO_2 to negligible concentration is a vital process that must be performed prior to liquefying natural gas (LNG) because it would prevent operational problems like freezing and clogging of cryogenic heat exchangers during natural gas liquefaction which occurs around −160 °C [2,3]. It also allows the liquefaction plant to be easily managed when there are process plant upsets at the upstream CO_2 capture plant. There are various technologies for capturing CO_2 like absorption, adsorption, membrane, cryogenic and microbial technology. However, the most proven and commercially available technology for CO_2 capture is by chemical absorption through the use of amine–based solvents [4,5]. Amine–based solvents are classified as primary (monoethanolamine, MEA), secondary (diethanolamine, DEA) and tertiary (methyldiethanolamine, MDEA) amines. Amine solvents known as sterically hindered amine (2–amino–2–methyl–1–propanol, AMP) and diamine (piperazine, PZ) have also been commonly used for CO_2 capture [6–8]. Furthermore, there are other problems associated with amine–based CO_2 which include high energy for amine solvent regeneration, foaming, and amine losses by vaporization [9–13]. Amine foaming issues are caused by the solubility of liquid hydrocarbons, organic acids and inhibitors, which can lead to reduced absorption capacity, amine carryover to downstream units and reduced mass transfer and efficiency [14–19]. However, Chakravarty et al. made the proposition that using blended amine solvents will maximize their CO_2 removal potentials [20]. Several experimental and pilot plant studies have reported improved CO_2 absorption–regeneration efficiency of blended amine solvents [21–25]. CO_2 removal from high pressure natural gas (i.e. natural gas sweetening) can be achieved using activated MDEA (aMDEA) which is a combination of MDEA as the base solvent and PZ as the activator.

The need to efficiently monitor, control and optimize the CO_2

* Corresponding authors.
E-mail addresses: nwaoha2c@uregina.ca, chikezienwaoha@live.co.uk (C. Nwaoha), kenneth.odoh@gmail.com (K. Odoh).

http://dx.doi.org/10.1016/j.jece.2017.10.038
Received 5 August 2017; Received in revised form 19 September 2017; Accepted 17 October 2017
Available online 18 October 2017
2213-3437/

Nomenclature

MDEA	Methyldiethanolamine
PZ	Piperazine
SG–CO_2	CO_2 flow rate in the sweet gas t/day
SG–MDEA	MDEA flow rate in the sweet gas, t/day
SG–PZ	PZ flow rate in the sweet gas, t/day
RA–C_5	Pentane flow rate in the CO_2 rich amine solution exiting the absorber, t/day
SG–C_1	Methane flow rate in the sweet gas exiting the absorber top, t/day
RAL	CO_2 rich amine loading, mol CO_2/mol amine
LAL	CO_2 lean amine loading, mol CO_2/mol amine
HD	Heat duty, GJ/hr
LAF	Lean amine flow rate, t/day
LAP	Lean amine pressure, bar
LAT	Lean amine temperature, °C
$C_{MDEA–PZ}$	MDEA–PZ concentration difference, wt.%
aMDEA	Activated MDEA, wt.%
OH^-	Hydroxyl ion
H_3O^+	Hydronium ion
HCO_3^-	Bicarbonate ion
CO_3^{2-}	Carbonate ion
$MDEAH^+$	Protonated MDEA
PZH_2^{2+}	Deprotonated PZ
PZH^+	Protonated PZ
$PZCOO^-$	PZ carbamate
H^+PZCOO^-	Protonated PZ carbamates
$PZ(COO^-)_2$	PZ dicarbamate

capture process plant has led to the use of process simulators and intelligent models. There are a number of process simulators which include Aspen HYSYS, Aspen Plus, and ProMax® while one of the intelligent models used is adaptive neuro–fuzzy inference system (ANFIS) [26–34,6].

The advantage of process simulators is that it does not require process plant historical data, hence can be used for initial design of process plants and to also optimize newly built process plants. Unlike process simulators, intelligent models make use of process plant historical data which can be very time–consuming and expensive to assemble. However, intelligent models are associated with very high predictive power and do not involve the application of complex thermodynamic theories and expression [32,34]. Therefore, both process simulator and intelligent models can be applied together towards process plant design and optimization.

The objective of this study is to use ProMax® 4.0 to model and validate CO_2 capture from high pressure natural gas, generate datasets consisting of dependent and independent process parameters and then conduct a parametric sensitivity analysis. ANFIS model will also be employed to predict the dependent process parameters. The independent process parameters are the lean amine pressure (LAP, bar), lean amine flow rate (LAF, t/day), lean amine temperature (LAT, °C), heat duty (HD, GJ/h), MDEA and PZ wt.% concentration difference ($C_{MDEA–PZ}$, wt.%). The dependent process parameters are CO_2 flow rate in the sweet gas (SG–CO_2, t/day), PZ flow rate in the sweet gas (SG–PZ, tonne/day), MDEA flow rate in the sweet gas (SG–MDEA, t/day), CO_2 rich amine loading (RAL, mol CO_2/mol amine), CO_2 lean amine loading (LAL, mol CO_2/mol amine), pentane (C_5) flow rate in the CO_2 rich amine solution (RA–C_5, t/day) and methane flow rate in the sweet gas (SG–C_1, t/day).

2. MDEA–PZ–CO_2–H_2O reaction chemistry

The absorption of CO_2 using amine–based solvents is analogous to an acid–base reaction, where the amine solvent is the base while CO_2 is the acid, to form salts like amine carbamates ($AmineCOO^-$), bicarbonates (HCO_3^-), etc. In this study, the chemical equilibria involve a bi–solvent blend containing MDEA and PZ and the various reactions between the amine solvents and CO_2 is detailed in Eqs. (1)–(11) [35–41]:

$$2H_2O \overset{k1}{\leftrightarrow} H_3O^+ + OH^- \quad (1)$$

$$CO_2 + 2H_2O \overset{k2}{\leftrightarrow} H_3O^+ + HCO_3^- \quad (2)$$

$$HCO_3^- + H_2O \overset{k3}{\leftrightarrow} H_3O^+ + CO_3^{2-} \quad (3)$$

$$MDEAH^+ + H_2O \overset{k4}{\leftrightarrow} MDEA + H_3O^+ \quad (4)$$

$$MDEA + CO_2 + H_2O \overset{k5}{\leftrightarrow} MDEAH^+ + HCO_3^- \quad (5)$$

$$PZH_2^{2+} + H_2O \overset{k6}{\leftrightarrow} PZH^+ + H_3O^+ \quad (6)$$

$$PZH^+ + H_2O \overset{k7}{\leftrightarrow} PZ + H_3O^+ \quad (7)$$

$$PZ + CO_2 + H_2O \overset{k8}{\leftrightarrow} PZCOO^- + H_3O^+ \quad (8)$$

$$PZCOO^- + CO_2 + H_2O \overset{k9}{\leftrightarrow} H^+PZCOO^- + HCO_3^- \quad (9)$$

$$H^+PZCOO^- + H_2O \overset{k10}{\longleftrightarrow} PZCOO^- + H_3O^+ \quad (10)$$

$$PZCOO^- + CO_2 + H_2O \overset{k11}{\longleftrightarrow} PZ(COO^-)_2 + H_3O^+ \quad (11)$$

A typical ionization reaction for aqueous systems that involves CO_2 is shown in Eqs. (1)–(3). The reaction between CO_2 and MDEA (of very low CO_2 absorption rate) does not produce $AmineCOO^-$ but generates HCO_3^- because MDEA is a tertiary amine solvent (Eqs. (4) and (5)) [35]. Hence, there is the need to use a polyamine activator (like PZ) to enhance the CO_2 absorption rate when a tertiary amine solvent is used. Eqs. (6)–(11) highlights the various reactions involving CO_2 and PZ. The presence of two secondary amino groups in PZ leads to the formation deprotonated PZ (PZH_2^{2+}) as well as PZ dicarbamate ($PZ(COO^-)_2$). The CO_2–amine species of PZ and MDEA are expected to complement each other towards enhancing their CO_2 absorption and regeneration performance. This is because the formation of HCO_3^- which is produced by MDEA favors regeneration while the formation of different carbamates of PZ increases the rate of CO_2 absorption.

3. Process simulation description

The natural gas sweetening plant using activated MDEA was simulated using ProMax® 4.0, and the natural gas composition used fall within the range of a typical Nigerian natural gas composition (Table 1) as made available by Gas Aggregation Company of Nigeria [42]. The activated MDEA in this study is a bi–solvent blend containing MDEA and PZ. Table 1 shows the process parameters used for modeling the CO_2 capture plant while Fig. 1 shows the process flowsheet of a typical natural gas sweetening plant.

The fluid property package chosen for the simulation was Amine Sweetening–Peng Robinson. This package was designed by Bryan Research & Engineering, Inc. for gas sweetening units. The Amine Sweetening property package accounts for non–ideal ionic interactions except at very high acid gas loadings (> 1 mol/mol) [43]. The absorber stage model and thermodynamic package were specified as, ideal stage and TSWEET Kinetics Model as recommended by ProMax® 4.0 licensors [43]. The TSWEET Kinetics Model predicts the amine–CO_2 kinetic reactions that occur in the absorber. The absorber and

Table 1
The detailed data used for the process simulation.

Parameters	Process data
Feed gas	
Gas composition (vol.%)	C_1 = 91.1 C_2 = 3.48 C_3 = 1.9 iC_4 = 0.4 nC_4 = 0.55 C_{5+} = 0.5 CO_2 = 2 H_2O = 0.07
Temperature	25 °C
Pressure	50 bar
Flow rate	450 MMSCFD
Lean amine	activated MDEA (aMDEA)
Total Amine Concentration	50 wt.% (MDEA = 45 wt.%; PZ = 5 wt.%)
Temperature	50 °C
Pressure	70 bar
Flow Rate	3900 t/day
Regenerator	
Reboiler Duty	55.5 GJ/h
Regenerator Pressure	1.6 bar
Condenser Temperature	30 °C

regenerator consist of 36 trays and 24 trays respectively and they were modeled with ideal/real stage ratio of '3' and '2' respectively. The absorber and regenerator diameters were specified (4 m and 3 m, respectively) while their tray spacing was kept at 0.6 m. The tray spacing was chosen based on previous studies which can be from 0.5 m to 0.76 m [44,45,6]. The column (absorber and regenerator) number of trays and diameters were varied constantly until the optimal condition was determined. The optimal condition is determined when there is little or no change in CO_2 absorption efficiency when the number of trays and column diameters were varied. In addition, a ProMax solver tool was implemented on the lean amine stream in order to determine the amine flow rate that will meet the target CO_2 specification in the sweet gas (2 ppm). This was done will varying the column (absorber and regenerator) diameter and tray number.

The pressure drop along the absorber column was fixed at 0.2 bar. The pressure of the CO_2 rich amine solution entering the flash drum was 9 bar and was achieved with the upstream valve. This allows most of the absorbed hydrocarbons to be flashed from the CO_2 rich amine solution thereby preventing hydrocarbons from entering the high temperature regenerator. The temperature approach in the lean/rich heat exchanger was specified as 10 °C in order to maximize the thermal efficiency of the heat exchanger. This temperature approach was achieved by implementing a ProMax solver option on the CO_2 rich amine stream exiting the lean/rich heat exchanger.

The stage model and thermodynamic package for the regenerator column was specified as ideal stage and TSWEET Stripper as recommended by ProMax® 4.0 licensors [43]. The system factor for both the absorber and regenerator was specified as 0.8, as this shows that there could be the possibility of foaming. The activated MDEA system for natural gas sweetening is usually a blend of MDEA and PZ (when blended with physical or chemical solvents) can be used up to 0.8 kmol/m^3 (about 7 wt.%) [5,46]. This is because PZ will precipitate when it is used at concentration above its room temperature (20 °C) solubility which is 1.4 kmol/m^3 or 14 wt.% [46–48]. Hence this study limited PZ concentration to maximum 7 wt.% to avoid any chances of precipitation. Therefore, for the base case simulation in this study the MDEA and PZ concentration was 45 wt.% and 5 wt.%, respectively since the total amine concentration is 50 wt.%. The natural gas composition used in this study contains 2 vol.% CO_2 which have to be reduced to 2 ppm (in the sweet gas) with minimum energy penalty. The amine concentration and CO_2 specification in the sweet gas was used for the validation of the simulation.

3.1. Data acquisition

Suitable data sets which cover the real–life distribution of input and output variables were integral to developing reliable models. The acquisition of suitable data sets for modeling allows the impact of input variables (independent process parameters) on output variables (dependent process parameters) to be observed. The datasets used in this study was generated from validated process simulation using the ProMax Scenario Tool®. The Scenario Tool® is an Excel add-in that is used as an Excel workbook embedded within the ProMax simulation

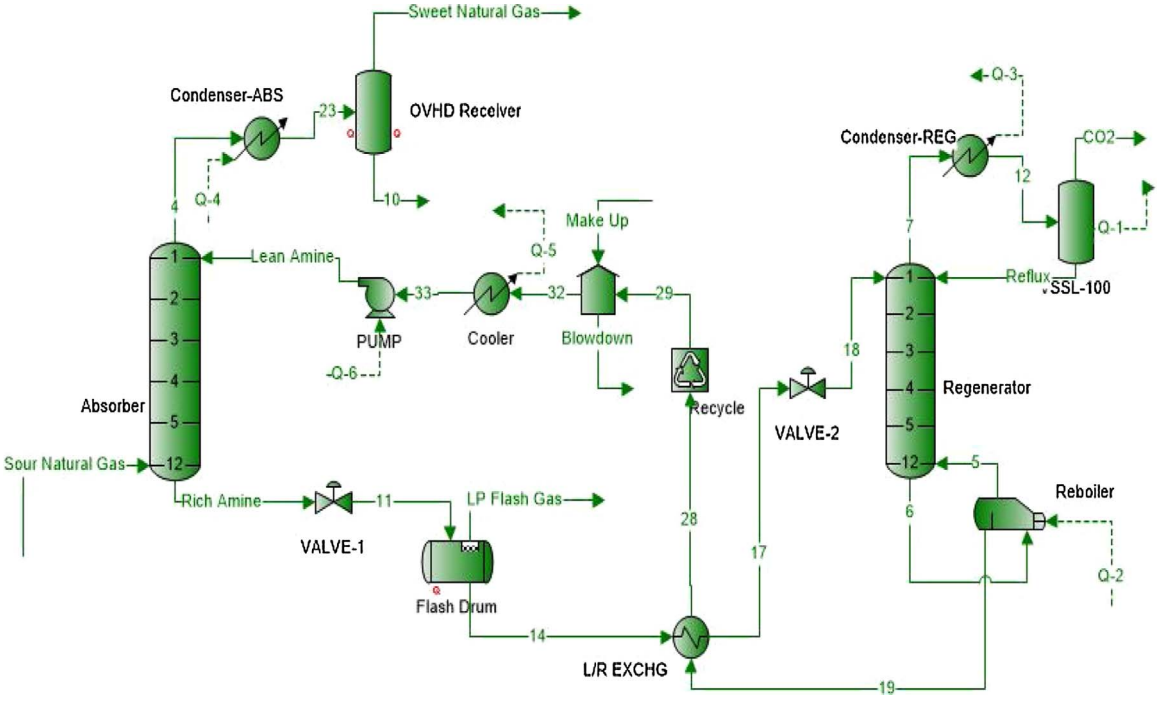

Fig. 1. Flowsheet of a typical natural gas sweetening plant.

Table 2
Input process parameters varied in the validated simulation.

Independent process parameters	Varied	Range
LAP (bar)	5	60; 63.75; 67.5; 71.25; 75
LAF (t/day)	5	3500; 3700; 3900; 4100; 4300
LAT (°C)	5	40; 45; 50; 55; 60
$C_{MDEA–PZ}$ (MDEA/PZ, wt.%)	5	43/7; 44/6; 45/5; 46/4; 47/3
Heat duty (GJ/h)	5	50.4; 51.93; 53.46; 54.99; 56.52
Total datasets generated	3125	

which allows independent process parameters (input parameters) to be specified and varied while monitoring results of various dependent process parameters [43]. Stepwise procedure for the Scenario Tool is provided in the Supplementary material. Table 2 shows the independent process parameters variables that were varied in the validated simulation.

4. Parametric sensitivity analysis and ANFIS modeling description

4.1. Parametric sensitivity analysis description

Parametric sensitivity analysis is integral in the optimizing process plant operation because it allows the contribution of various process parameters on the plant efficiency to be determined and quantified. For this study, considering that the independent process parameters (LAP, LAF, LAT, HD and $C_{MDEA–PZ}$) have different units and scale, they were normalized to between 0 and 1 using the correlation in Eq. (12). This was done to make it easier to identify which independent process parameter was most important.

$$x_{norm} = \frac{x - x_{min}}{x_{max} - x_{min}} \tag{12}$$

Where; x_{norm} is the normalized value of the process parameter, x is the actual value of the process parameter, x_{min} is the minimum value of the process parameter while x_{max} is the maximum value of the process parameter.

The normalized independent process parameters (x–axis) were then plotted in a graph against their corresponding value of the dependent process parameter (y–axis). The graph is intended to reveal if the independent process parameter has a linear or inverse effect on the dependent process parameter (y–axis). The slope of the graph indicates the contribution or magnitude of the independent process parameter on the dependent process parameter. When more than one independent process parameters are studied (like in this case) the slope of the graph can be used to compare which independent process parameters have the highest and least impact on the dependent process parameter.

Fig. 2 displays scenarios where the normalized independent process parameters can assume either a linear, exponential, logarithmic, polynomial or a combination of these trends. It is important to note that the slopes of logarithmic, exponential and polynomial curves are different at different points of the plot. In such cases, the slope of the adjacent points is taken, after which the final slope will be the geometric mean or log–mean average of the adjacent point's slopes.

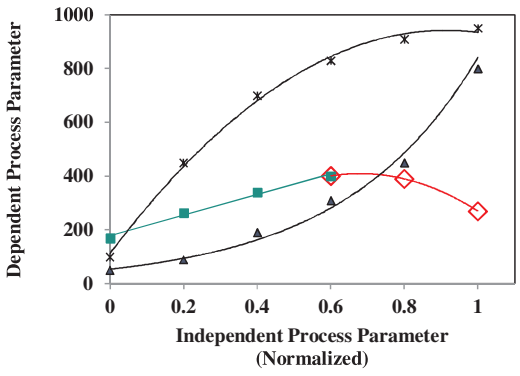

Fig. 2. Normalized independent process parameters plotted against dependent process parameter showing different scenarios.

It is also observed (Fig. 2) that there could be cases where both an increase and decrease regions (green and red curves) will exist on a particular curve. For such scenarios the plot can be split into the different regions, and then the slope of each region is determined. This is important because it will reveal which region has the highest impact on the dependent process parameter. In order to compare such independent process parameter with other independent process parameters, a single slope will be determined. The single slope value is determined by adding the absolute values of the different regions slopes.

For this analysis, as one independent process parameter is varied, other independent process parameters were kept constant, and their effect on various dependent process parameters were recorded. The independent process parameters were varied at MDEA–PZ concentration of 45 wt.%–5 wt.% which was the concentration used to validate the simulation. Fig. 3 depicts the flow chart for conducting the parametric sensitivity analysis.

Another advantage of this method of parametric sensitivity analysis is that it allows more than one independent process parameter to be plotted in a single graph against a particular dependent process parameter.

4.2. ANFIS model description

ANFIS is an intelligent model that was introduced by [49], It combines the high learning capabilities of a neural network with the modeling ability of fuzzy logic to capture uncertainties in the data, thereby resulting in a model with a high predictive power. This is a fuzzy-based inference system based on adaptive neural network that

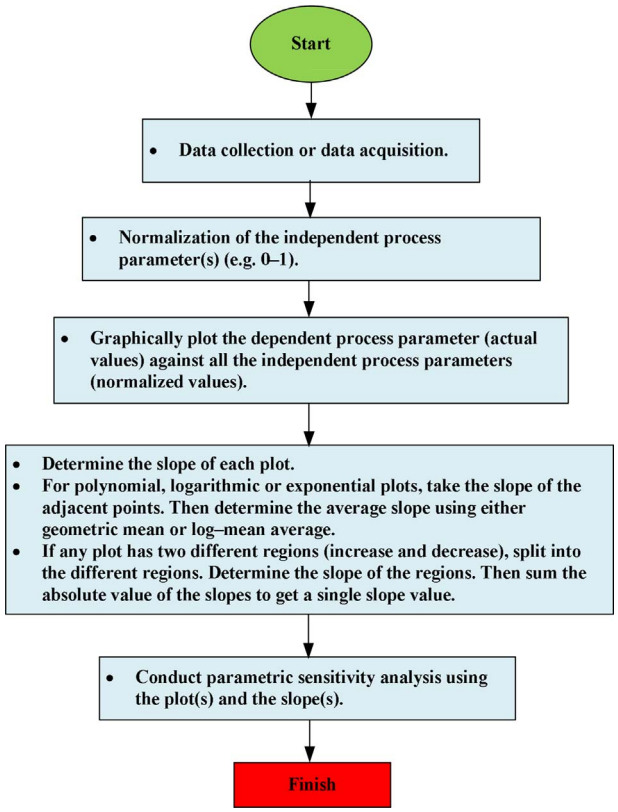

Fig. 3. Step-wise parametric sensitivity analysis flow chart.

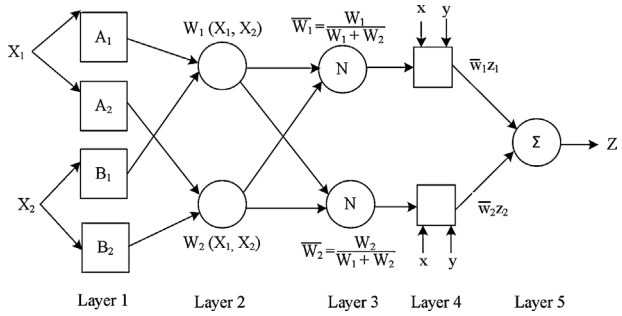

Fig. 4. ANFIS architecture for a two input variables and one output variable.

can model non-linear relationships in the data, and has proven useful for prediction of chaotic time series. ANFIS uses a unique learning procedure that combines gradient descent and least square to reduce the likelihood of getting stuck in local minima, thereby guarantying getting to the optima minima [50,49]. The learning in ANFIS employs a two pass procedure in every epoch which consists of forward pass and backward pass. The parameters for each node are obtained in the forward pass that comes from the input. The error rate is propagated from output to the input using the gradient descent [49]. In ANFIS, the network and fuzzy inference system is trained by a neural network to obtain the fuzzy representation. Any correctly designed ANFIS can solve any nonlinear and complex problems with high predictive power [51]. Fig. 4. displays the ANFIS architecture.

As shown in Fig. 4, ANFIS has five layers, two inputs x, and y and an output z, Fig. 4. The first-order Sugeno fuzzy model can be represented using the following rules:

Rule 1: if x is A_1 and y is B_1, then $z_1 = p_1{*}x + q_1{*}y + r_1$

Rule 2: if x is A_2 and y is B_2, then $z_2 = p_2{*}x + q_2{*}y + r_2$

Rule 3: if x is A_1 and y is B_2, then $z_3 = p_3{*}x + q_3{*}y + r_3$

Rule 4: if x is A_2 and y is B_1, then $z_4 = p_4{*}x + q_4{*}y + r_4$

In the above rules, p_1, p_2, p_3, p_4, q_1, q_2, q_3, q_4, r_1, r_2, r_3, r_4 are the parameters and the linguistic labels are A_1, B_1, A_2, and B_2.

Layer 1: This layer provides the mapping of the input variables x, y to fuzzy set {A_1, A_2, B_1, B_2}. This transition is done using a membership function.

Layer 2: The aim of this layer is to derive firing strength from fuzzy conjunction of the input. This results in the multiplication of the input to produce an output. This is represented by $W_1(x, y)$ and $W_2(x, y)$.

Layer 3: This layer provides the ratio of ith firing strength to the summation of firing strength. This is the normalization of the firing strength across the levels. This is represented by $W_1(x, y)$ and $W_2(x, y)$.

Layer 4: This layer performs multiplication of the output from Layer 3 using a function of Sugeno fuzzy rule. This is represented by Eqs. (13) and (14).

$$\overline{W_1} = \frac{W_1}{W_1 + W_2} \tag{13}$$

$$\overline{W_2} = \frac{W_2}{W_1 + W_2} \tag{14}$$

Layer 5: This is the output layer which is the summation of the output from Layer 4. This uses a weighted average to perform defuzzification to transform the fuzzy set into real-world output [52]. Table 3 shows the system parameters used for the ANFIS modeling.

The data preprocessing used in this project normalizes the data to have the range between 0.1 and 0.9 and this reduces the effect of scale differences in the data set. This does not affect the accuracy of the prediction as the effect of scaling can be captured by the weights and biases of the nodes, thereby not influencing the overall output. This results in faster training times of the ANFIS network [53]. The ANFIS model is a Python implementation named ANFIS [54] and was evaluated using cross-validation. Cross-Validation is the process of

Table 3
System parameters for the ANFIS modeling.

Parameter	Description/value
Structure	Takagi-Sugeno
Membership	Gaussian
Number of inputs	7
Number of Outputs	6
Training method	Hybrid (back propagation with least square estimation)

randomly splitting the data set into K sets of roughly equal sizes. Only one of the K sets is held out for testing. The remaining K-1 sets are for training the model. The held-out set are predicted using the trained model and for estimation of performance measures. The benefit of cross-validation is that it prevent over fitting of the data, which can lead to unrealistic estimation [55]. The choice of K is based on a trade-off between computational power, variance, and bias. The lower values of K would require cheaper computational resources, lower variance, and higher bias. The higher values of K would require more computational resources, higher variance, and lower bias. The choice of 5-fold cross validation was chosen for this study for evaluating the performance of ANFIS model [55].

4.3. Statistical error analysis

The accuracy and precision of the model was determined by using the statistical measures which include absolute average deviation (%AAD) and root mean square error as shown in Eqs. (15) and (16). High accuracy and precision is achieved when%AAD and RMSE are both close to zero. The%AAD was also used for validation of the CO_2 capture plant simulation.

$$\%\mathrm{AAD} = \frac{100}{n}\sum_{i=1}^{n}\left|\frac{P_i - N_i}{N_i}\right| \tag{15}$$

$$\mathrm{RMSE} = \left(\frac{1}{n}\sum_{i=1}^{n}(P_i - N_i)^2\right)^{0.5} \tag{16}$$

Where: 'n' is the sample size, 'N_i' is the actual value from simulation and 'P_i' is the ANFIS predicted value.

5. Amine foaming tendency determination

Foaming is one of the major problems encountered during CO_2 and H_2S removal from natural gas streams. This is usually caused by amine degradation products, dissolved liquid hydrocarbons (C_{5+}), organic acids and inhibitors [14–18]. Foaming leads to reduced absorption capacity, amine carryover to downstream units, reduced mass transfer and efficiency [19]. This study predicted amine foaming tendency by the flow rate of the absorbed C_5 (pentane flow rate) in the CO_2 rich amine solution (RA–C_5) exiting the absorber bottom. This method was chosen because C_5 is a liquid hydrocarbon and absorbed liquid hydrocarbons by amine solvents lead to amine foaming. Therefore, the higher the absorbed C_5 in the CO_2 rich amine solution is, the higher the tendency of amine foaming.

6. Amine loss by vaporization determination

Amine loss by vaporization is one of the major challenges of CO_2 capture plants. This is because it can lead to additional amine costs, reduced CO_2 capture efficiency in the absorber and introduces impurities in the treated gas, have environmental implications, and pose a threat to human health and aquatic life [11,13]. All these contribute to increased operating costs. This study analyzed the vaporization losses of MDEA and PZ using their flow rate in the sweet gas (SG–MDEA and

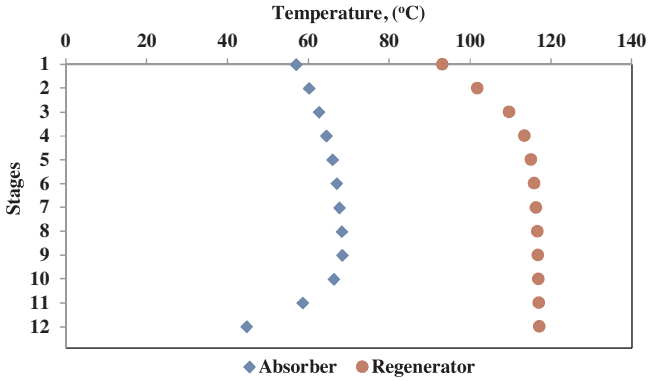

Fig. 5. Absorber and regenerator temperature profiles of the base case (45 wt.% MDEA–5 wt.% PZ) simulation.

SG–PZ). An increase in SG–MDEA and SG–PZ translates to an increase to MDEA and PZ losses through vaporization.

7. Results and discussion

7.1. ProMax® 4.0 simulation validation

The initial step prior to conducting parametric sensitivity analysis and ANFIS modeling is to validate the natural gas sweetening simulation. One of the best approaches to validating simulation results is to use the temperature profile in the absorber and regenerator. The absorber temperature profile reveals the exothermic trend of amine–CO_2 reaction and an increase in temperature indicate where the absorption rate is highest [56]. For CO_2 capture systems containing high MDEA concentrations (≥30 wt.% MDEA), the temperature bulge is located towards the bottom of the absorber [57–62]. This trend is also replicated by the MDEA–PZ simulation in this study (Fig. 5). In addition, the regenerator temperature profile for amine–CO_2 system is usually highest at the bottom (slightly linear from the bottom to the center) and reduces a bit sharply towards the top [63,7,64]. This was also the trend observed in this study as shown in Fig. 5. Hence, the simulation is accurately validated and results can be used for further study and analysis.

7.2. Parametric sensitivity analysis

Parametric sensitivity analysis was carried out in this study to investigate the effect of various process parameters (independent process parameters), namely, lean amine pressure (LAP), lean amine flow rate (LAF), lean amine temperature (LAT), heat duty (HD) and MDEA–PZ weight concentration difference ($C_{MDEA–PZ}$) on various dependent process parameters. The dependent process parameters were CO_2 flow rate in the sweet gas (SG–CO_2), PZ flow rate in the sweet gas (SG–PZ), MDEA flow rate in the sweet gas (SG–MDEA,), CO_2 rich amine loading (RAL), CO_2 lean amine loading (LAL), pentane (C_5) flow rate in the CO_2 rich amine solution (RA–C_5) and methane flow rate in the sweet gas (SG–C_1). The C_5 flow rate in the CO_2 rich amine solution is used to determine foaming tendency while the MDEA and PZ flow rate in the sweet gas were used to estimate amine emissions during CO_2 absorption.

7.2.1. Lean amine loading (LAL)

The LAL is a key process parameter because low LAL is associated with higher CO_2 absorption efficiency [65]. Fig. 6 reveals that both the LAT and LAP have no significant effect on LAL, though LAL increases with an increase in LAP.

Fig. 6 shows that as HD increases the LAL decreases; this is because increasing the HD will enhance the breakdown of amine carbamates ($AmineCOO^-$), protonated amines ($AmineH^+$) and bicarbonate ions (HCO_3^-) in the CO_2 rich amine solution. Previous studies also confirmed this trend [28,66–68,21]. It is also confirmed that LAL has a linear relationship with the LAF. This is because at high LAL, more LAF will be required effective CO_2 capture. This has been confirmed in the literature [69,70,67,28]. It is important to note that an increased LAF is not entirely desired because it usually leads to increased HD for regeneration. On the effect of $C_{MDEA–PZ}$ on LAL, it was observed (Fig. 6) that as $C_{MDEA–PZ}$ decreased, the LAL also increased. A decrease in $C_{MDEA–PZ}$ translates to lower concentration of MDEA and higher PZ concentration. In such scenario, the PZ–CO_2 interaction will increase while the MDEA–CO_2 interaction will decrease leading to lower HCO_3^- concentration and increased PZ carbamates in the CO_2 rich amine solution. This is consistent with reported data in the literature [28,22]. Amine carbamates are more difficult to breakdown during regeneration as compared to HCO_3^-. The process parameters' contributions to the LAL rank in the order $C_{MDEA–PZ}$ > LAF > HD > LAT > LAP. Therefore, the first three process parameters ($C_{MDEA–PZ}$, LAF and HD) are integral towards optimizing the LAL, but cost implications usually determines which process parameter to consider first. Cost implications here refer to increase in operating cost when there are increases in amine solvent concentration, lean amine pumping and energy input.

7.2.2. Rich amine loading (RAL)

It is desirable for a process plant to be optimized in order to obtain a high RAL or to make the amine solution reach its maximum CO_2 loading capacity (equilibrium loading). This will translate to reducing the CO_2 flow rate in the sweet gas (SG–CO_2) [65]. Hence, there is need to have a good understanding of how various process variables affect the RAL. Fig. 7 shows the relationship between different process parameters and the RAL. It can be seen that HD and LAF have inverse relationship with the RAL, whereas LAT, LAP and $C_{MDEA–PZ}$ have a linear relationship with RAL. However, LAP, HD and LAT can be said to have no significant contribution to the RAL because of their negligible

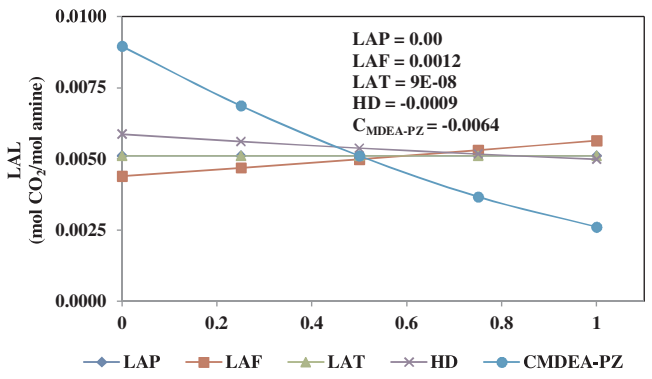

Fig. 6. Effect and contribution of various process parameters on LAL.

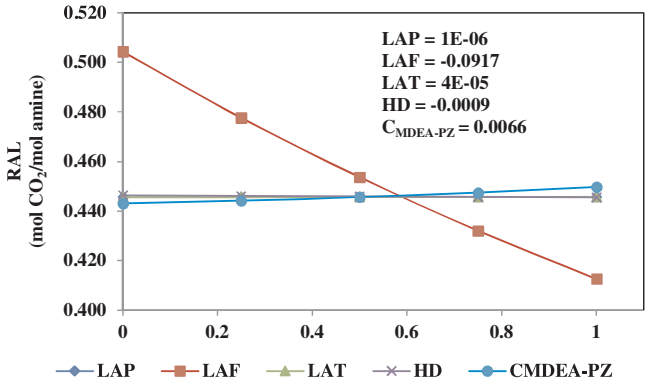

Fig. 7. Effect and contribution of various process parameters on RAL.

slopes.

Fig. 7 reveals that the LAF by far has the highest influence towards RAL and an increase in LAF leads to a decrease in RAL. This relationship has also been obtained in previous as well as in recent studies [71,65,70,69]. This trend is beneficial because reducing the LAF while maintaining the SG–CO_2 minimizes the cost of pumping and sensible heat during amine regeneration. The linear relationship between $C_{MDEA–PZ}$ and the RAL is because of the competing effects of kinetics and solubility. As the $C_{MDEA–PZ}$ effect increases from 0 to 1 the RAL increases indicating that solubility (MDEA contribution) took priority than kinetics (PZ contribution). It is also important to remember that CO_2 loading increases as amine molar concentration reduces and this is the case as $C_{MDEA–PZ}$ increases from 0 to 1.

The HD is inversely related to the RAL as seen in Fig. 7. This scenario have been demonstrated in a previous study [65]. Fig. 7 also shows that increasing the LAT led to a slight increase in the RAL. An increase in LAT decreases the viscosity of the lean amine solution but increases the overall volumetric mass transfer coefficient [72,73]. This can make solubility to take priority above kinetics within the temperature ranges studied, and hence the higher RAL. The competing effect between solubility and kinetics due to LAT has been previously reported [74]. Increase in RAL due to an increase in LAT has also been reported in the literature [75]. This highlights that in order to optimize RAL, the most important parameter is LAF followed by $C_{MDEA–PZ}$. Since LAF has an inverse relationship with RAL, it is therefore important to improve CO_2 capture efficiency at the lowest possible LAF. The influence of the process parameters is in the order LAF > $C_{MDEA–PZ}$ > HD > LAT > LAP.

7.2.3. Amine vaporization losses

Amine losses through vaporization is a big issue in CO_2 capture plants because it leads to increased capital and operating costs, environmental implications, as well as threats to human health and aquatic life [11,13]. Capital cost will increase due to the requirement of larger water wash units whereas the operating cost will increase due to increased amine make–up especially for very expensive amine solvents. Also, in terms of the environment, this can be detrimental due to possible toxicity of the amine solvents [13,11]. Figs. 8 and 9 reveals the relationship between various process parameters towards MDEA and PZ flow rates in the sweet gas (SG–MDEA and SG–PZ).

From Figs. 8 and 9, only the LAT and $C_{MDEA–PZ}$ have significant effect on both SG–MDEA and SG–PZ. As the LAT increased (within the studied temperature range) the SG–MDEA and SG–PZ increased. This can be attributed to the fact that as LAT increases, the vaporization of both MDEA and PZ increases, This is more evident in PZ. The low atmospheric boiling point of PZ (145 °C) as compared to MDEA (246 °C) is another reason for the higher SG–PZ when LAT is increased. It can be seen from Fig. 8 that as the $C_{MDEA–PZ}$ increases the SG–MDEA increases. This is because an increase in MDEA concentration will lead to more

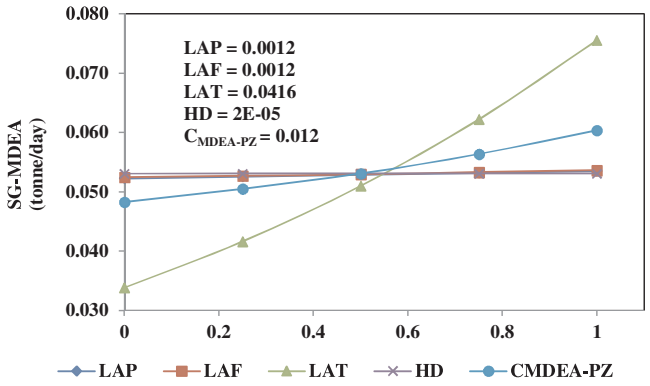

Fig. 8. Effect and contribution of various process parameters on SG–MDEA.

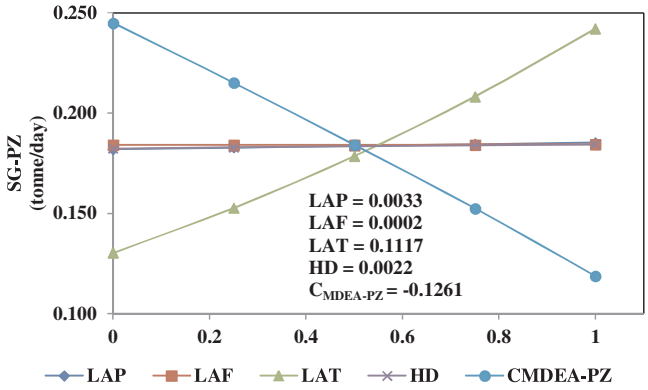

Fig. 9. Effect and contribution of various process parameters on SG–PZ.

MDEA vaporization and carryover with the sweet gas. On the other hand as $C_{MDEA–PZ}$ increases the SG–PZ decreases (Fig. 9). This is because an increase in $C_{MDEA–PZ}$ translates to a decrease in PZ concentration. The reduction in PZ concentration reduces the carryover of PZ with the sweet gas. However, the effect of $C_{MDEA–PZ}$ was discovered to have much more influence on SG–PZ than on the SG–MDEA (Figs. 8 and 9).

The HD has a linear relationship with both SG–MDEA and SG–PZ; however, this effect is also more dominant in SG–PZ whereas there is no significant effect to SG–MDEA (Figs. 8 and 9). This is because increasing the HD decreases LAL (Fig. 6), and a decrease in LAL means there is more free amines (PZ and MDEA) available during CO_2 absorption, and hence increased amine carryover with the sweet gas (SG–PZ than to SG–MDEA). The effect of CO_2 loading on amine volatility has been confirmed in the literature [11]. Unlike the HD, the LAF has more influence on SG–MDEA than SG–PZ (Figs. 8 and 9). The linear relationship between LAF and both SG–MDEA than SG–PZ is because an increase in LAF increases the amount of amine (MDEA and PZ) molecules in the absorber, hence the increased amine carryover. The effect of process parameters towards SG–MDEA is ranked in the order LAT > $C_{MDEA–PZ}$ > LAF ~ LAP > HD. For that of SG–PZ they are follow the rank $C_{MDEA–PZ}$ > LAT > LAP > HD > LAF.

7.2.4. CO_2 flow rate in sweet gas (SG–CO_2)

The SG–CO_2 is required to be very low in order to meet sales gas specification and to also avoid possible solidification in cryogenic heat exchangers during natural gas liquefaction. Fig. 10 displays the effect of process parameters on the SG–CO_2. It can be seen that the LAP, LAT and HD all have inverse relationships with the SG–CO_2 while the LAF has a linear relationship with the SG–CO_2. For $C_{MDEA–PZ}$ two regions can be seen consisting of both linear and inverse relationship (Fig. 10).

Ordinarily, increasing LAF (increase in liquid/gas flow rate ratio) increases both the effective interfacial area and liquid mass transfer coefficient, hence higher CO_2 capture and removal [76,65,77–79,6,71].

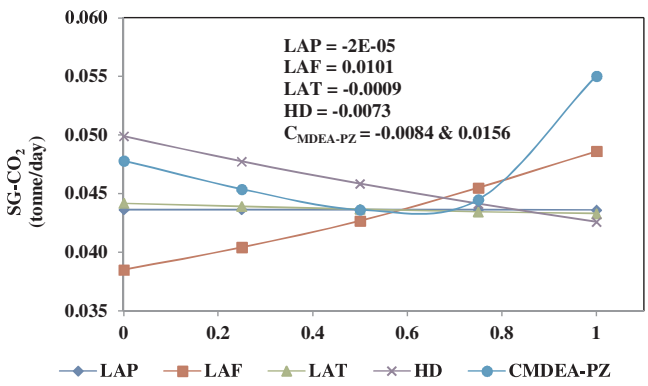

Fig. 10. Effect and contribution of various process parameters on SG–CO_2.

However, very high flow rates becomes counter–productive because it creates bubbles which reduce the effective interfacial area between CO_2 and active amine molecules, and hence reduced mass transfer. This scenario is the case in this study as can be seen in Fig. 10; as the LAF increases, the SG–CO_2 increases. Increasing the HD increased CO_2 absorption efficiency (lower CO_2 flow rate in the sweet gas) as seen in Fig. 10 and was also stated previously in literatures [79,65,67]. This trend is true because at higher HD the LAL reduces (Fig. 6) thereby allowing for increased CO_2 absorption.

The SG–CO_2 reduced when LAT is increased because an increase in temperature (within the temperature range of this study) increases both the rate of reaction and the overall mass transfer coefficient [80,72]. Previous as well as recent studies have also reported the same trend for LAT towards CO_2 capture efficiency [77,7,74,81,31]. This is also beneficial because higher LAT means less energy for cooling the lean amine entering the absorber; but it is important to note that LAT is also related to the temperature of the sweet gas. Higher sweet gas temperature might lead to a larger energy for cooling the sweet gas most especially if the gas is to be liquefied. Another challenge is that continuous increase in LAT can become counter–productive and lead to an increase in the SG–CO_2 [7,74,31]. Also, very a high temperature in the absorber can accelerate corrosion which is not desired.

Though increasing LAP reduced CO_2 flow rate in the sweet gas (increased CO_2 absorption), it has no significant effect on SG–CO_2. This is particularly good because increasing LAP will increase operating cost due to higher pumping energy. The effect of increasing the absorber column pressure was also confirmed by previous researchers [65,28,78]. It is noticed from Fig. 10 that as $C_{MDEA–PZ}$ increases, the SG–CO_2 decreases at a particular region and then increases in another region. This nonlinearity is because when the $C_{MDEA–PZ}$ effect decreased from 1 to 0.5 the effect of both PZ–CO_2 interactions (kinetics) and solubility dominated and hence, leading to increased CO_2 absorption efficiency (reduced SG–CO_2). A similar trend has also been reported in the literature for CO_2 absorption and H_2S absorption [65,76,78]. Other activators (monoethanolamine, MEA and diethanolamine, DEA) blended with MDEA also showed the same trend [68]. Though viscosity increased as the $C_{MDEA–PZ}$ decreased from 1 to 0.5 it posed no limitation on both solubility and kinetics.

On the other hand when the $C_{MDEA–PZ}$ further decreased from 0.5 to 0 the CO_2 absorption efficiency decreased (increased SG–CO_2), though PZ concentration is highest at 0. This can be because kinetics (PZ) took priority as opposed to solubility (in MDEA). This can also be because the increase in viscosity when $C_{MDEA–PZ}$ decreased from 0.5–0 affected mass transfer of CO_2 into the liquid phase. Also, when PZ concentration is maximum ($C_{MDEA–PZ}$ is 0) the PZ vaporization is high (Fig. 9), hence affecting the PZ contribution to CO_2 absorption. The effect of process variables towards the SG–CO_2 are in this order $C_{MDEA–PZ}$ > LAF > HD > LAT > LAP.

7.2.5. Amine foaming

Amine foaming during CO_2 capture from natural gas stream is mainly caused by inhibitors, organic acids and solubility of liquid hydrocarbons which can then lead to amine carryover to downstream units, reduction in absorption capacity, as well as reduced mass transfer and efficiency [14–19]. In this study, amine foaming was predicted using the flow rate of pentane (C_5) in the CO_2 rich amine solution exiting the absorber bottom (RA–C_5).

Fig. 11 shows that LAT, LAP and HD have no significant effect on the RA–C_5 though they have a linear relationship with RA–C_5. The linear relationship is because an increase in LAP increases solubility driving force, hence increasing the absorption of C_5. On the other hand, increasing HD reduces LAL which increases absorption efficiency. The effect of HD on absorption efficiency can be noticed for SG–CO_2 (Fig 10). However, the effect of HD on SG–CO_2 outperforms its effect on RA–C_5. Previous researchers confirmed that solubility and pickup of light hydrocarbons by amine solvents increases with amine

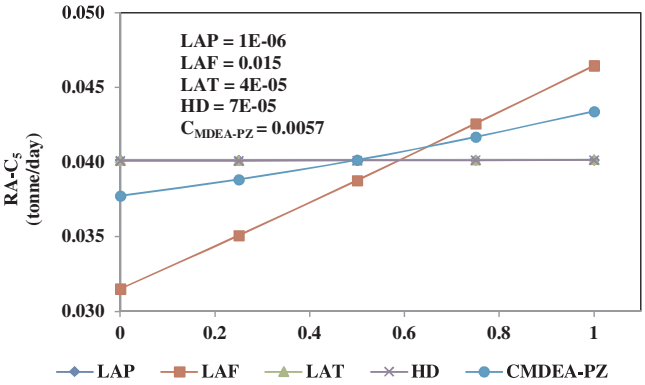

Fig. 11. Effect and contribution of various process parameters on RA–C_5.

concentration [9,10]. This is also related to this study in which an increase $C_{MDEA–PZ}$ increased RA–C_5 (Fig. 11). This also means that, an increase in MDEA concentration with a corresponding decrease in PZ concentration increased RA–C_5. It can be related to the fact that an increase in $C_{MDEA–PZ}$ reduced LAL (Fig. 6) and a reduced LAL increases absorption.

The LAF has a linear relationship with RA–C_5 and it also has the highest effect compared to other process parameters. This is because increasing LAF increases the active amines in the absorber, hence increasing the absorption of C_5. Similar trend has been previously reported [9]. The influence of different process parameters towards RA–C_5 is ranked as LAF > $C_{MDEA–PZ}$ > HD > LAT > LAP.

7.2.6. Methane flow rate in the sweet gas (SG–C_1)

Co–absorption of methane (C_1) by amine solution is not desired in natural gas sweetening because it reduces the amount of the desired product produced, hence affecting the cash flow of the plant. Fig 12 displays the influence of various process parameters on the SG–C_1.

Fig. 12 reveals that LAF, HD and $C_{MDEA–PZ}$ have inverse relationships with SG–C_1, but the LAF has the highest impact compared to other process parameters. This effect of LAF is because as LAF increases more active amines are available, hence increasing C_1 co–absorption which in turn decreases the SG–C_1. Similar trend was noticed for LAF effect on RA–C_5; however, the effect of LAF is higher on RA–C_5 than on SG–C_1. An increase in HD decreased the SG–C_1 because increasing the HD leads to a decrease in LAL which in turn allows more absorption of methane in the CO_2 rich amine solution. The more the methane absorbed, the lower the methane flow rate in the sweet gas. It is also important to state that though increasing HD decreases SG–C_1, its effect towards decreasing SG–CO_2 is very dominant ((Figs. 11 and 12)). In addition, an increase in $C_{MDEA–PZ}$ reduced the SG–C_1 which indicates that MDEA contributes more to methane absorption than PZ. This is because an increase in $C_{MDEA–PZ}$ means a decrease in PZ concentration and a corresponding increase in MDEA concentration.

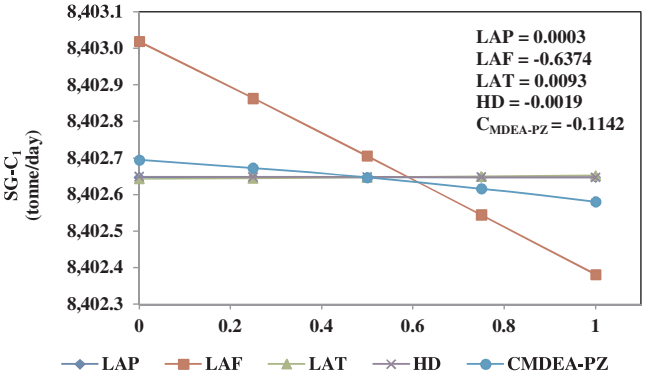

Fig. 12. Effect and contribution of various process parameters on SG–C_1.

On the other hand, the LAP and LAT have linear relationships with SG–C_1, and the LAP has the lowest impact. This is because increasing LAT shifts the absorption temperature farther above the dew point temperature of C_1 which then reduces its solubility and condensation in the amine solution. It can also be because since increase in LAT increases CO_2 absorption (Fig. 11), then this will reduce the methane absorption efficiency of the amine solution. It is also believed the LAP effect on SG–C_1 followed the same trend since increase in LAP increases CO_2 absorption efficiency (Fig. 11). The influence of different process parameters towards SG–C_1 is ranked as LAF > $C_{MDEA-PZ}$ > LAT > HD > LAP.

8. ANFIS prediction

The prediction ability of ANFIS based model for the dependent process parameters are shown in the parity plots (Figs. 13–19). The

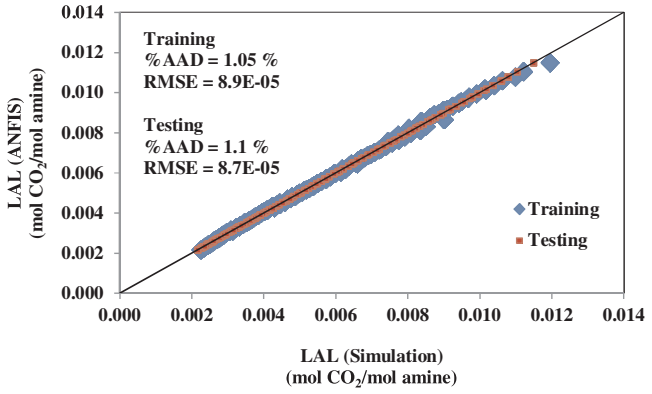

Fig. 13. Parity plot of LAL for both training and testing datasets.

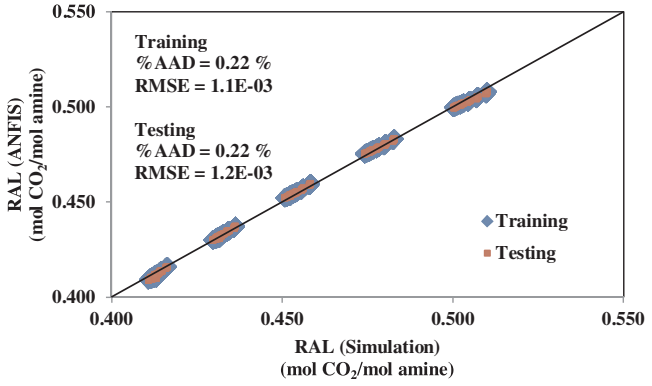

Fig. 14. Parity plot of RAL for both training and testing datasets.

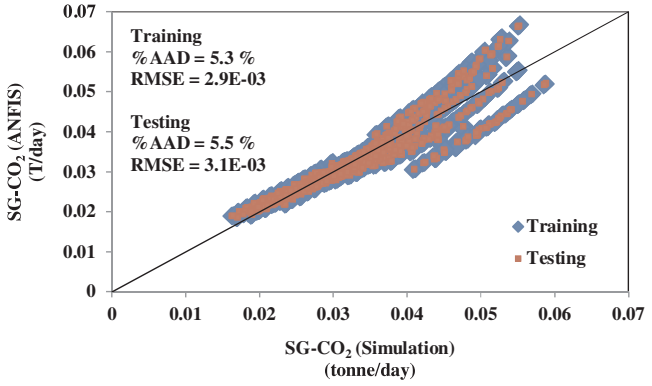

Fig. 15. Parity plot of SG–CO_2 for both training and testing datasets.

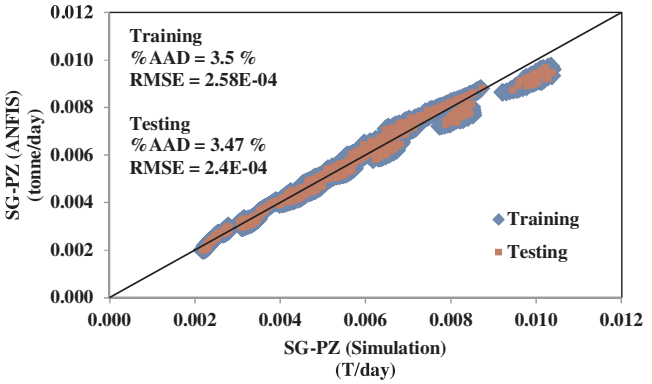

Fig. 16. Parity plot of SG–PZ for both training and testing datasets.

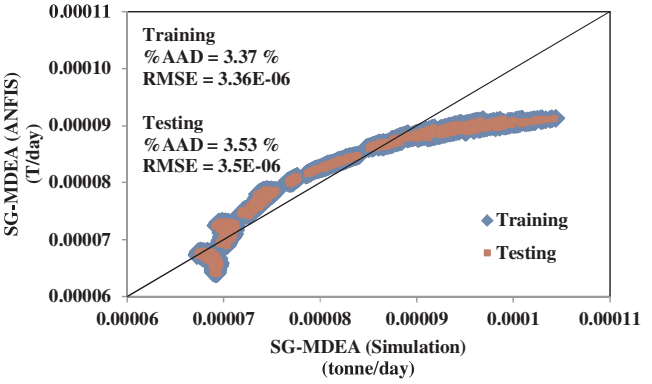

Fig. 17. Parity plot of SG–MDEA for both training and testing datasets.

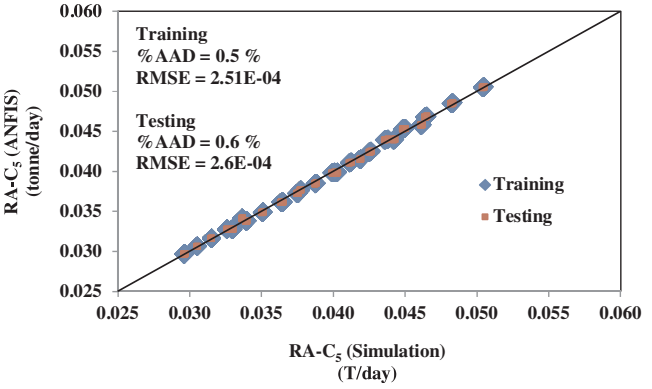

Fig. 18. Parity plot of RA–C_5 for both training and testing datasets.

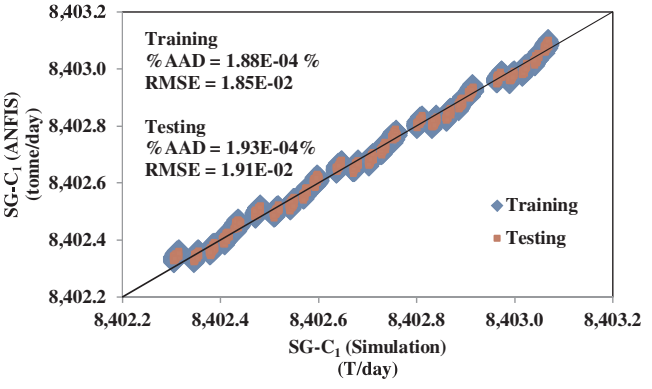

Fig. 19. Parity plot of SG–C_1 for both training and testing datasets.

results from both training and testing datasets are plotted in same graph. The training was carried out with 70% of the entire datasets (2187 datasets) while 30% (938 unused datasets) was used for the testing. The statistical parameters for determining accuracy and precision indicate that ANFIS model accurately predicted the actual values of the various dependent process parameters very well (Figs. 13–19).

9. Conclusions

- Results showed that the LAP has no effect on the LAL, whereas LAT and LAF linearly related to the LAL while the HD and $C_{MDEA–PZ}$ had an inverse effect on the LAL. The process parameters influence to the LAL rank in the order: $C_{MDEA–PZ}$ > LAF > HD > LAT > LAP.
- From the results of this study, the impact of the independent process parameters on RAL is in the order: LAF > $C_{MDEA–PZ}$ > HD > LAT > LAP, while the influence of the independent process parameters towards the SG–CO_2 are in this order: $C_{MDEA–PZ}$ > LAF > HD > LAT > LAP.
- The LAF has the highest impact on amine foaming tendency (RA–C_5) followed by $C_{MDEA–PZ}$ while the LAP has the lowest contribution.
- Methane flow rate in the sweet gas (SG–C_1) increases with increasing LAF and LAP while increasing LAF, HD and $C_{MDEA–PZ}$ reduces SG–C_1. Their effect towards SG–C_1 followed the trend: LAF > $C_{MDEA–PZ}$ > LAT > HD > LAP.
- The influence of the investigated independent process parameters on SG–MDEA and SG–PZ followed the order LAT > $C_{MDEA–PZ}$ > LAP ~ LAF > HD and $C_{MDEA–PZ}$ > LAT > LAP > HD > LAF respectively.
- The parametric sensitivity analysis revealed that $C_{MDEA–PZ}$ and LAF are very influential towards optimizing CO_2 absorption efficiency, maintaining high natural gas production rate, while controlling amine emissions and foaming. However, LAP is the least influential parameter. This observation is based on the range of the independent process parameters studied in this work.
- The well trained ANFIS model accurately predicted all the dependent process parameters with maximum%AAD and RMSE of 2.4% and 4.0E-03, respectively.

Acknowledgements

The authors gratefully thank Clean Energy Technologies Research Institute (CETRI), Faculty of Engineering and Applied Science, University of Regina–CANADA for providing access to the process simulator (ProMax® 4.0) used for this research work.

Appendix A. Supplementary data

Supplementary data associated with this article can be found, in the online version, at https://doi.org/10.1016/j.jece.2017.10.038.

References

[1] British Petroleum, "Energy Outlook 2035,", British Petroleum (BP), 2016.
[2] S. Mokhatab, J. Mak, J. Valappil, D.A. Wood, LNG plant and regasification terminal operations, Handbook of Liquefied Natural Gas, 1st ed., Gulf Professional Publishing, 2014, pp. 297–320 Gulf Professional Publishing is an imprint of Elsevier.
[3] J. Goodchild, T. Lind, A. Melville, Pretreatment system modifications for improving CO2 removal in the feedgas for 3 gas utility peak-shaving plants, LNG 17 International Conference & Exhibition on Liquefied Natural Gas, Houston, 2013.
[4] A.B. Rao, E.S. Rubin, A technical, economical, and environmental assessment of amine based CO2 capture technology for power plant greenhouse gas control, Environ. Sci. Technol. 36 (20) (2002) 4467–4475.
[5] A. Kohl, R. Nielsen, Gas Purification, 5th ed., Gulf Publishing, Texas, 1997.
[6] M.S. Jassim, Sensitivity analyses and optimization of a gas sweetening plant for hydrogen sulfide and carbon dioxide capture using methyldiethanolamine solutions, J. Nat. Gas Sci. Eng. 36 (2016) 175–183.
[7] U. Zahid, F.N. Al Rowaili, M.K. Ayodeji, U. Ahmed, Simulation and parametric analysis of CO2 capture from natural gas using diglycolamine, Int. J. Greenh. Gas Control 57 (2017) 42–51.
[8] A.A. Khan, G.N. Halder, A.K. Saha, Comparing CO2 removal characteristics of aqueous solutions of monoethanolamine, 2-amino-2-methyl-1-propanol, methyldiethanolamine and piperazine through absorption process, Int. J. Greenh. Gas Control 50 (2016) 179–189.
[9] J.A. Bullin, W.G. Brown, Hydrocarbons and btex pickup and control from amine systems, Presented at the 83rd Annual GPA Convention (2004).
[10] J.J. Carroll, J. Maddocks, A.E. Mather, The solubility of hydrocarbons in amine solutions, Laurance Reid Gas Conditioning Conference, Norman, Oklahoma USA, 1998.
[11] T. Nguyen, M. Hilliard, G.T. Rochelle, Amine volatility in CO2 capture, Int. J. Greenh. Gas Control 4 (2010) 707–715.
[12] R. Idem, M. Wilson, P. Tontiwachwuthikul, A. Chakma, A. Veawab, A. Aroonwilas, D. Gelowitz, Pilot plant studies of the CO2 capture performance of aqueous MEA and mixed MEA/MDEA solvents at the university of regina CO2 capture technology development plant and the boundary dam CO2 capture demonstration plant, Ind. Eng. Chem. Res. 45 (2006) 2414–2420.
[13] C. Nwaoha, T. Supap, R. Idem, C. Saiwan, P. Tontiwachwuthikul, M.J. AL-Marri, A. Benamor, Advancement and new perspectives of using formulated reactive amine blends for post-combustion carbon dioxide (CO2) capture technologies, Petroleum 3 (2017) 10–36.
[14] Y. Ke, B. Shen, H. Sun, J. Liu, X. Xu, Study on foaming of formulated solvent UDS and improving foaming control in acid natural gas swetening process, J. Nat. Gas Sci. Eng. 28 (2016) 271–279.
[15] C.R. Pauley, Face the facts about amine foaming, Chem. Eng. Prog. 87 (7) (1991) 33–38.
[16] C.R. Pauley, Ways to control amine unit foaming offered, Oil Gas J. 87 (50) (1989) 67–75.
[17] Emerson Process Management, Avoiding Amine Foaming Issues Utilizing a Gas Chromatograph, Emerson Process Management, 2012.
[18] I. Ratman, T.D. Kusworo, A.F. Ismail, Foam behaviour of an aqueous solution of piperazine- N-Methyldiethanolamine (MDEA) blend as a function of the type of impurities and concentrations, Int. J. Sci. Eng. 1 (1) (2010) 7–14.
[19] X. Chen, S.A. Freeman, G.T. Rochelle, Foaming of aqueous piperazine and monoethanolamine for CO2 capture, Int. J. Greenh. Gas Control 5 (2) (2011) 381–386.
[20] T. Chakravarty, U.K. Phukan, R.H. Weiland, Reaction of acid gases with mixtures of amines, Chem. Eng. Prog. 81 (1985) 32–36.
[21] Y. Artanto, J. Jansen, P. Pearson, G. Puxty, A. Cottrell, E. Meuleman, P. Feron, Pilot-scale evaluation of AMP/PZ to capture CO2 from flue gas of an Australian brown coal–fired power station, Int. J. Greenh. Gas Control 20 (2014) 189–195.
[22] C. Nwaoha, C. Saiwan, P. Tontiwachwuthikul, T. Supap, W. Rongwong, R. Idem, M.J. AL-Marri, A. Benamor, Carbon dioxide (CO2) capture: absorption-desorption capabilities of 2-amino-2-methyl-1-propanol (AMP), piperazine (PZ) and monoethanolamine (MEA) tri-solvent blends, J. Nat. Gas Sci. Eng. 33 (2016) 742–750.
[23] C. Nwaoha, C. Saiwan, T. Supap, R. Idem, P. Tontiwachwuthikul, W. Rongwong, M.J. AL-Marri, A. Benamor, Carbon dioxide (CO2) capture performance of aqueous tri-solvent blends containing 2-amino-2-Methyl-1-propanol (AMP) and methyldiethanolamine (MDEA) promoted by diethylenetriamine (DETA), Int. J. Greenh. Gas Control 53 (2016) 292–304.
[24] F.A. Chowdhury, K. Goto, H. Yamada, Y. Matsuzaki, S. Yamamoto, T. Higashii, M. Onoda, Results of RITE's advanced liquid absorbents develop for low temperature CO2 capture, Energy Procedia, (2017).
[25] A.A. Khan, G.N. Halder, A.K. Saha, Experimental investigation on efficient carbon dioxide capture using piperazine (PZ) activated aqueous methyldiethanolamine (MDEA) solution in a packed column, Int. J. Greenh. Gas Control 64 (2017) 163–173.
[26] H. Gao, L. Zhou, Z. Liang, R. Idem, K. Fu, T. Sema, P. Tontiwachwuthikul, Comparative studies of heat duty and total equivalent work of a new heat pump distillation with split flow process, conventional split flow process, and conventional baseline process for CO2 capture using monoethanolamine, Int. J. Greenh. Gas Control 24 (2014) 87–97.
[27] A.S. Berrouk, R. Ochieng, Improved performance of the natural gas sweetening Benfield-HiPure process using process simulation, Fuel Process. Technol. 127 (2014) 20–25.
[28] B. Zhao, F. Liu, Z. Cui, C. Liu, H. Yue, S. Tang, Y. Liu, H. Lu, B. Liang, Enhancing the energetic efficiency of MDEA/PZ-based CO2 capture technology for a 650 MW power plant: process improvement, Appl. Energy 185 (2017) 362–375.
[29] J. Yu, S. Wang, H. Yu, Experimental studies and rate-based simulations of CO2 absorption with aqueous ammonia and piperazine blended solutions, Int. J. Greenh. Gas Control 50 (2016) 135–146.
[30] N.M.A. Al-Lagtah, S. Al-Habsi, S.A. Onaizi, Optimization and performance improvement of Lekhwair natural gas sweetening plant using Aspen HYSYS, J. Nat. Gas Sci. Eng. 26 (2015) 267–381.
[31] B. Pouladi, M.N. Hassankiadeh, F. Behroozshad, Dynamic simulation and optimization of an industrial-scale absorption tower for CO2 capturing from ethane gas, Energy Rep. 2 (2016) 54–61.
[32] M.M. Ghiasi, M. Arabloo, A.H. Mohammadi, T. Barghi, Application of ANFIS soft computing technique in modeling the CO2 capture with MEA, DEA, and TEA aqueous solutions, Int. J. Greenh. Gas Control 49 (2016) 47–54.
[33] A. Tatar, A. Barati-Harooni, A. Najafi-Marghmaleki, A. Mohebbi, M.M. Ghiasi, A.H. Mohammadi, A. Hajinezhad, Comparison of two soft computing approaches for predicting CO2 solubility in aqueous solution of piperazine, Int. J. Greenh. Gas Control 53 (2016) 85–97.
[34] Q. Zhou, C.W. Chan, P. Tontiwachwuthikul, R. Idem, D. Gelowitz, Application of neuro-fuzzy modeling technique for operational problem solving in a CO2 capture process system, Int. J. Greenh. Gas Control 15 (2013) 32–41.
[35] G. Sartori, D.W. Savage, Sterically hindered amines for CO2 removal from gases,

Ind. Eng. Chem. Fundam. 22 (1983) 239–249.
[36] M. Kundu, S.S. Bandyopadhyay, Solubility of CO2 in water + diethanolamine + N-methyldiethanolamine, Fluid Phase Equilib. 248 (2006) 158–167.
[37] T.L. Donaldson, Y.N. Nguyen, Carbon dioxide reaction kinetics and transport in aqueous amine membrane, Ind. Eng. Chem. Fundam. 19 (3) (1980) 260–266.
[38] A. Samanta, S.S. Bandyopadhyay, Kinetics and modeling of carbon dioxide absorption into aqueous solutions of piperazine, Chem. Eng. Sci. 62 (2007) 7312–7319.
[39] P.J. Derks, C. Kleingeld, C. van Aken, J.A. Hogendoorn, G.F. Versteeg, Kinetics of absorption of carbon dioxide in aqueous piperazine solutions, Chem. Eng. Sci. 61 (2006) 6837–6854.
[40] S. Bishnoi, G.T. Rochelle, Absorption of carbon dioxide into aqueous piperazine: reaction kinetics, mass transfer and solubility, Chem. Eng. Sci. 55 (2000) 5531–5543.
[41] J.M. Plaza, G. Rochelle, Modeling pilot plant results for CO2 capture by aqueous piperazine, Energy Procedia 4 (2011) 1593–1600.
[42] Gas Aggregation Company of Nigeria, National Gas Specification, (2016) ([Accessed 17 July 2016]. [Online]. Available: http://www.gacn.com/wp-content/uploads/2016/10/DownloadNationalgasspec.pdf).
[43] Bryan Research & Engineering, ProMax® 4.0, Bryan Research & Engineering Inc., USA, Texas, 2017.
[44] S.S. Warudkar, K.R. Cox, M.S. Wong, G.J. Hirasaki, Influence of stripper operating parameters on the performance of amine absorption systems for post-combustion carbon capture: part I. High pressure strippers, Int. J. Greenh. Gas Control 16 (2013) 342–350.
[45] A. Aboudheir, W. Elmoudir, Optimization of an existing 130 tonne per day CO2 capture plant from a flue gas slipstream of a coal power plant, Energy Procedia 37 (2013) 1509–1516.
[46] M. Appl, U. Wagner, H.J. Henrici, K. Kuessner, K. Volkamer, E. Fuerst, Removal of CO2 and/or H2 S and/or COS from gases containing these constituents, Patent US 4336233 A, 22 June 1982.
[47] S.A. Freeman, R. Dugas, D. Van Wagener, T. Nguyen, G.T. Rochelle, Carbon dioxide capture with concentrated, aqueous piperazine, Energy Procedia, (2009).
[48] S.A. Freeman, R. Dugas, D.H. Van Wagener, T. Nguyen, G.T. Rochelle, Carbon dioxide capture with concentrated, aqueous piperazine, Int. J. Greenh. Gas Control 4 (2010) 119–124.
[49] J.R. Jang, ANFIS: Adaptive-network-based fuzzy inference system, IEEE Trans. Syst. Man Cybernet. 23 (3) (1993) 665–685.
[50] A. Barati-Harooni, A. Najafi-Marghmaleki, A.H. Mohammadi, ANFIS modeling of ionic liquids densities, J. Mol. Liq. 224 (2016) 965–975.
[51] A. Kamari, A.H. Mohammadi, M. Lee, T. Mahmood, A. Bahadori, Decline curve based models for predicting natural gas well performance, Petroleum 3 (2) (2017) 242–248.
[52] A. Zendehboudi, X. Li, B. Wang, Utilization of ANN and ANFIS models to predict variable speed scroll compressor with vapour injection, Int. J. Refrig. 74 (2017) 475–487.
[53] T. Raiko, H. Valpola, Y. Lecun, Deep learning made easier by linear transformations in perceptrons, J. Mach. Learn. Res. 22 (2012) 924–932.
[54] M. Tim, Python Implementation of an Adaptive Neuro Fuzzy Inference System, (2015) ([Accessed 10 January 2017] [Online] Available: https://github.com/twmeggs/anfis).
[55] R. Kohavi, A study of cross-validation and bootstrap for accuracy estimation and model selection, Proceedings of the 14th International Joint Conference on Artificial Intelligence, San Francisco USA, 1995.
[56] H.M. Kvamsdal, G.T. Rochelle, Effects of the Temperature Bulge in CO2 absorption from flue gas by aqueous monoethanolamine, Ind. Eng. Chem. Res. 47 (2008) 867–875.
[57] E. Solbraa, Equilibrium and Non-Equilibrium Thermodynamics of Natural Gas Processing, (2002) Trondheim, Norway.
[58] S. Moioli, L.A. Pellegrini, B. Picutti, P. Vergani, Improved rate-Based modeling of H2S and CO2 removal by methyldiethanolamine scrubbing, Ind. Eng. Chem. Res. 52 (2013) 2056–2065.
[59] P. Blauwhoff, B. Kamphuis, W. Van Swaaij, K.R. Westerterp, Absorber design in sour natural gas treatment plants: impact of process variables on operation and economics, Chem. Eng. Process. Process Intensif. 19 (1985) 1–25.
[60] H. Zare Aliabad, S. Mirzaei, Removal of CO2 and H2S using aqueous alkanolamine solusions, Int. J. Chem. Mol. Nucl. Mater. Metall. Eng. 3 (1) (2009) 50–59.
[61] T. Borhani, M. Afkhamipour, A. Azarpour, V. Akbari, S.H. Emadi, Z.A. Manan, Modeling study on CO2 and H2S simultaneous removal using MDEA solution, J. Ind. Eng. Chem. 34 (2016) 344–355.
[62] A. Shahsavand, A. Garmroodi, Simulation of Khangiran gas treating units for various cooling scenarios, J. Nat. Gas Sci. Eng. 2 (2010) 277–283.
[63] J.P. Gutierrez, L.A. Benitez, E.L. Ale Ruiz, E. Erdmann, A sensitivity analysis and a comparison of two simulators performance for the process of natural gas sweetening, J. Nat. Gas Sci. Eng. 31 (2016) 800–807.
[64] B.-H. Li, N. Zhang, R. Smith, Simulation and analysis of CO2 capture process with aqueous monoethanolamine solution, Appl. Energy 161 (2016) 707–717.
[65] S.K. Dash, A.N. Samanta, S.S. Bandyopadhyay, Simulation and parametric study of post combustion CO2 capture process using (AMP + PZ) blended solvent, Int. J. Greenh. Gas Control 21 (2014) 130–139.
[66] C. Alie, L. Backham, E. Croiset, P.L. Douglas, Simulation of CO2 capture using MEA scrubbing: a flow sheet decomposition method, Energy Convers. Manage. 46 (2005) 475–487.
[67] M.R.M. Abu-Zahra, L.H.J. Schneiders, J.P.M. Niederer, P.H.M. Feron, G.F. Versteeg, CO2 capture from power plants: part I. A parametric study of the technical performance based on monoethanolamine, Int. J. Greenh. Gas Control 1 (1) (2007) 37–46.
[68] W.A. Fouad, A.S. Berrouk, Using mixed tertiary amines for gas sweetening energy requirement reduction, J. Nat. Gas Sci. Eng. 11 (2013) 12–17.
[69] R. Notz, H.P. Mangalapally, H. Hasse, Post combustion CO2 capture by reactive absorption: pilot plant description and results of systematic studies with MEA, Int. J. Greenh. Gas Control 6 (2012) 84–112.
[70] H.P. Mangalapally, H. Hasse, Pilot plant study of two new solvents for post combustion carbon dioxide capture by reactive absorption and comparison to monoethanolamine, Chem. Eng. Sci. 66 (2011) 5512–5522.
[71] M. Bui, I. Gunawan, V. Verheyen, P. Feron, E. Meuleman, Flexible operation of CSIRO's post-combustion CO2 capture pilot plant at the AGL Loy Yang power station, Int. J. Greenh. Gas Control 48 (2016) 188–203.
[72] K. Fu, T. Sema, Z. Liang, H. Liu, Y. Na, H. Shi, R. Idem, P. Tontiwachwuthikul, Investigation of mass-transfer performance for CO2 absorption into diethylenetriamine (DETA) in a randomly packed column, Ind. Eng. Chem. Res. 51 (2012) 12058–12064.
[73] B. Xu, H. Gao, X. Luo, H. Liao, Z. Liang, Mass transfer performance of CO2 absorption into aqueous DEEA in packed columns, Int. J. Greenh. Gas Control 51 (2016) 11–17.
[74] J.A. Bullin, J.C. Polasek, S.T. Donnelly, The use of MDEA and mixtures of amines for bulk CO2 removal, Proceedings of the Sixty-Ninth GPA Annual Convention Tulsa, OK: Gas Processors, Tulsa, OK, 1990.
[75] H. Cho, M. Binns, K.-J. Min, J.-K. Kim, Automated process design of acid gas removal units in natural gas processing, Comput. Chem. Eng. 83 (2015) 97–109.
[76] O. Younas, F. Banat, Parametric sensitivity analysis on a GASCO's acid gas removal plant using ProMax simulator, J. Nat. Gas Sci. Eng. 18 (2014) 247–253.
[77] I.P. Koronaki, L. Prentza, V.D. Papaefthimiou, Parametric analysis using AMP and MEA as aqueous solvents for CO2 absorption, Appl. Therm. Eng. 110 (2017) 126–135.
[78] S. Mudhasakul, H.-M. Ku, P.L. Douglas, A simulation model of a CO2 absorption process with methyldiethanolamine solvent and piperazine as an activator, Int. J. Greenh. Gas Control 15 (2013) 134–141.
[79] N. Rodríguez, S. Mussati, N. Scenna, Optimization of post-combustion CO2 process using DEA–MDEA mixtures, Chem. Eng. Res. Des. 89 (9) (2011) 1763–1773.
[80] J. Gao, J. Yin, F. Zhu, X. Chen, M. Tong, W. Kang, Y. Zhou, J. Lu, Postcombustion CO2 capture using diethylenetriamine (DETA) solvent in a pilot-plant test bed compared to monoethanolamine (MEA) solvent, Environ. Progress Sustain. Energy 17 (2017).
[81] L. Addington, C. Ness, An Evaluation of General Rules of Thumb in Amine Sweetening Unit Design and Operation, Bryan Research and Engineering, Inc., Texas USA, 2010.